Applied Medical Informatics
Original Research Vol. 39, No. 3-4 /2017, pp: 49-66

Power Spectral Analysis of Short-Term Heart Rate Variability in Healthy and Arrhythmia Subjects by the Adaptive Continuous Morlet Wavelet Transform

Ram Sewak SINGH[1*], Barjinder Singh SAINI[2], Ramesh Kumar SUNKARIA[2]

[1]Department of Electronics and Communication Engineering, IMS Engineering College Ghaziabad, Uttar Pradesh, India.
[2]Department of Electronics and Communication Engineering, Dr. B.R. Ambedkar National Institute of Technology, Jalandhar, Punjab, India.
E-mails: ramsewaknitj@gmail.com; sainibs@nitj.ac.in; sunkariark@nitj.ac.in

* Author to whom correspondence should be addressed; Tel.: +91955556167; Fax: +91-181-2690320

Received: December 3, 2018 /Accepted: December 19, 2017/ Published online: December 31, 2017

Abstract
Power spectral analysis of short-term heart rate variability (HRV) can provide instant valuable information to understand the functioning of autonomic control over the cardiovascular system. In this study, an adaptive continuous Morlet wavelet transform (ACMWT) method has been used to describe the time-frequency characteristics of the HRV using band power spectra and the median value of interquartile range. Adaptation of the method was based on the measurement of maximum energy concentration. The ACMWT has been validated on synthetic signals (i.e. stationary, non-stationary as slow varying and fast changing frequency with time) modeled as closest to dynamic changes in HRV signals. This method has been also tested in the presence of additive white Gaussian noise (AWGN) to show its robustness towards the noise. From the results of testing on synthetic signals, the ACMWT was found to be an enhanced energy concentration estimator for assessment of power spectral of short-term HRV time series compared to adaptive Stockwell transform (AST), adaptive modified Stockwell transform (AMST), standard continuous Morlet wavelet transform (CMWT) and Stockwell transform (ST) estimators at statistical significance level of 5%. Further, the ACMWT was applied to real HRV data from Fantasia and MIT-BIH databases, grouped as healthy young group (HYG), healthy elderly group (HEG), arrhythmia controlled medication group (ARCMG), and supraventricular tachycardia group (SVTG) subjects. The global results demonstrate that spectral indices of low frequency power (LFp) and high frequency power (HFp) of HRV were decreased in HEG compared to HYG subjects ($p<0.0001$). While LFp and HFp indices were increased in ARCMG compared to HEG ($p<0.00001$). The LFp and HFp components of HRV obtained from SVTG were reduced compared to other group subjects ($p<0.00001$).

Keywords: Adaptive continuous Morlet wavelet transform; Energy concentration measurement; Global method; Shape parameter

Introduction

Sustained arrhythmias are the most common reason of sudden cardiac death, about 75- 85 % cases each year in the world wide population [1]. The term arrhythmia refers to a disorder in the timing or pattern of the heartbeat. Arrhythmia may be due to abnormalities in impulse formation or in the heart's electrical system, or both, but it is not always a disorder of heart rhythm [2,3].

Respiratory sinus arrhythmia is a normal oscillation of heart rate, reflecting respiratory action. Impulse formation may be sinus or ectopic, the rhythm regular or irregular and the heart rate faster (> 100 beats per minute i.e. tachycardia), or slow (< 60 beats per minute i.e. bradycardia)[4,5]. Depending on primary disease conditions related to heart some arrhythmias are: heart block, atrial fibrillation, supraventricular tachycardia (SVT) and ventricular atrial fibrillation. Because of arrhythmia, the heart may beat inefficiently, and the body may receive an inadequate blood supply. This can cause symptoms and can be life-threatening [6,7].

From the QRS complex of Electrocardiogram (ECG) records, R-R intervals is measured, the beat to beat variation of R-R interval is known as heart rate variability (HRV). The HRV signals are non-stationary time-varying signals from a statistical perspective. Therefore, time-variant signal processing methods are part of the standard assortment in biomedical signal analysis. The time-frequency analysis of the HRV has been used as a non-invasive tool to explain the several mechanisms of the autonomic nervous system (ANS) modulating the heart rate [8]. The variation of power spectra of HRV signals in time-frequency domain has a high diagnostic value leading to more frequent applications of the time-variant analysis method [9, 10]. It is significant to obtain information about how power of the HRV is distributed across frequency and time.

The dynamic characteristics of HRV are measure of the balance between sympathetic and parasympathetic mediators (both are branches of ANS) of heart rate. Sympathetic mediator is initiated from influence of epinephrine and norepinephrine chemical messengers (neurotransmitters). These chemicals are released from sympathetic nerve fiber and act on sino-artial node (SAN) and atrioventricular node AVN[11]. These increase the rate of cardiac contraction and accelerate electrical system at the (AVN), leading to increase heart rate. Sympathetic mediators appear to exert their effect over longer times and are replicated in the low frequency (LF) band (0.04 to 0.15 Hz) of HRV[12]. In this band, power spectral distribution is known by LFp [13]. Parasympathetic mediator is initiated from effect of acetylcholine chemical neurotransmitter, is released from parasympathetic nerve fiber, and acts on SAN and AVN, which slows the rate of cardiac contraction of AVN, leading to decrease in heart rate. Parasympathetic mediators employ their effect more quickly on the heart and are reflected in the high frequency (HF) band (0.15 to 0.4 Hz), the spectral power distribution in HF band is represented by HFp of HRV[14]. Thus, the power spectral analysis is performed on the HRV data to show vagal tone and the sympatho-vagal balance as LFp/HFp ratio at any point of instant [15-17].

Power spectrum estimation of sampled time series signal is usually based on procedures employing the fast Fourier transform (FFT).This approach is computationally efficient and provides an excellent frequency resolution [18]. However, it does not tell anything about time series localization of the frequency components present in the signals. This reality has not effect on stationary signal, but real life signals are non-stationary like HRV, arterial blood pressure variability, arterial pulse interval variability and respiratory signals.

In an ideal case, the time-frequency mapping provides only information about the frequency occurring at a given instant of time without cross-information about adjacent instant [19, 20]. The most important aim of a time-frequency analysis method is to be close to ideal case and have excellent resolution [21]. The energy concentration related with resolution in the time-frequency analysis is one of its most important and severely studied aspects in time-frequency analysis of HRV signals [22]. Various popular methods like short time Fourier transform (STFT), wavelet transform and Stockwell transform (ST) exist for linear time-frequency analysis of HRV signals [9].

In STFT, a sliding and fixed duration window is introduced in Fourier integral to get a better estimation of localization of time of each frequency component [23]. Whereas, this improvement is obtained at the expense of frequency resolution due to fixed duration window [24]. The multiresolution technique overcomes the problem of STFT. In multiresolution concept, the fixed duration widow function of STFT is replaced by introducing translation and dilation of basis function, known as the mother wavelet function[25]. If the mother wavelet function is Morlet function (it is a plane wave modulated by Gaussian function), the multiresolution technique is known as standard continuous Morlet wavelet transform (CMWT). By using multiresolution strategy, it provides fixed number of cycles per dilation and resolution remains stationary along the dilation. However, in some cases, the CMWT suffers from poor energy concentration in the time frequency

domain at the higher frequencies, as higher and lower frequencies depend on highest analyzed frequency relative to lower frequency.

The standard ST is becoming a popular method for time-frequency analysis of non-stationary signals due to its simplicity and ability to preserve the phase information of signals [26]. The ST is a linear time-frequency analysis, which can be viewed as combination of STFT and CMWT. Because of this hybrid strategy, it enables the use of frequency variables and multiresolution strategy of continuous wavelets analysis. The Gaussian window function of ST depends on frequency; hence the ST produces excellent frequency resolution at lower frequencies and sharper time localization at higher frequencies [18, 27]. The characteristic of window function changes with frequency and not with time, thus the ST method is inappropriate for resolving signals, whose spectral components are fast changing with time [28]. Other reformed method of ST transform like adaptive Stockwell transform (AST) and modified Stockwell transform (MST) improved the energy concentration from ST by adding some parameter that controls the shape or frequency scale of its Gaussian window [29-31]. The parameter that controls the shape of window only improves the limited energy concentration of signals, whose fast frequency changes with time but not for all type of non-stationary (slow and rapid changing spectral) signals.

In this paper, we present adaptive methods that provide enhanced energy concentration for synthetic individual characteristics of HRV signal in time-frequency domain. The enhancement is accomplished through an additional parameter q, which controls the shape of Gaussian function used in time frequency transform. The q_{opt}parameter is calculated through an optimization strategy that maximizes the energy concentration of time-frequency estimator. All the dynamic characteristics of HRV modeled from the synthetic signals have been analyzed using four standard estimators CMWT, ST, AST, adaptive modified Stockwell transform (AMST) and also by using adaptive continuous Morlet wavelet transform (ACMWT). The adaptation of AST, AMST and ACMWT methods are based on maximum energy concentration measurement (ECMmax). To the extent of our knowledge these adaptive methods has never been used in the assessment of power distribution in LF and HF range of HRV signals. Further, ACMWT method is applied to estimate the power spectral in HRV signals of each group of subjects.

Material and Method

Standard Continuous Morlet Wavelet Transform

The standard CMWT of a time series signal $s_t$defined as

$$W_t(a,\tau) = \langle a, \psi_{a,\tau} \rangle = \frac{1}{\sqrt{a}} \int_{-\infty}^{+\infty} s_t \, \psi^* \left(\frac{t-\tau}{a}\right) dt \quad (1)$$

where ψ^*(t)is the complex conjugate of the mother wavelet ψ(t), which is the mother analysis wavelet function, a is the real positive number, denotes the scaling parameter of the mother wavelet and τ is also a real number, which shifts the scaled mother wavelet alongside the time axis [25]. The Morlet wavelet is a good example of a mother wavelet function for the building of the continuous wavelet transform. It consist of a plane wave modulated by Gaussian [32], the Morlet wavelet function is defined in time domain as:

$$\psi_M(t) = \pi^{-\frac{1}{4}} \left[e^{-iw_o t} - e^{-\frac{w_0^2}{2}} \right] e^{-\frac{t^2}{2}} \quad (2)$$

Its Fourier transform is defined in equation in (3), shifted Gaussian function and satisfies the admissibility condition so that $\hat{\psi}_M(0) = 0$

$$\hat{\psi}_M(w) = \pi^{-\frac{1}{4}} \left[e^{-\frac{(w-w_O)^2}{2}} - e^{-\frac{w_0^2+w^2}{2}} \right] \quad (3)$$

where w_0 is the central frequency of the mother wavelet. In this paper we have used $w_0 = 6$ for satisfy the admissible condition [21]and second term of equation (2) and (3) can be neglected in practice. The equation of Morlet wavelet function and its Fourier transform becomes

$$\psi_M(t) = \pi^{-\frac{1}{4}} e^{-iw_o t} e^{-\frac{t^2}{2}} \quad (4)$$

$$\hat{\psi}_M(w) = \pi^{-\frac{1}{4}} e^{-\frac{(w-w_o)^2}{2}} \quad (5)$$

Fourier transform of scaled by '*a*' of mother Morlet wavelet function written as

$$\hat{\psi}_M(a\,w) = \pi^{-\frac{1}{4}} e^{-\frac{(a\,w-w_o)^2}{2}} \quad (6)$$

While equation (2) satisfies the requirements to be a wavelet function if mean of equation (4) is approximately zero. The mean of wavelet function calculated as

$$\int_{-\infty}^{+\infty} \psi_M(t)\ dt = \sqrt{2}\,\pi^{-\frac{1}{4}} e^{-\frac{{w_o}^2}{2}} \quad (7)$$

Hence, the value of mean is so small for $w_0 > 5$ that it satisfies the zero mean wavelet.

The CMWT improved the energy concentration by introducing a γ shape parameter to the Gaussian part of Morlet wavelet function, which balances the time and frequency resolution[33]. The γ shape parameter is a function of frequency. Thus, the Morlet wavelet function of equation (4) becomes as

$$\psi_M(t,\gamma) = \pi^{-\frac{1}{4}} e^{-iw_o t} e^{-\frac{\gamma^2 t^2}{2}} \quad (8)$$

As γ is function of frequency, hence γ (f) = 1/f and equation (8) becomes

$$\psi_M(t,\gamma(f)) = \pi^{-\frac{1}{4}} e^{-iw_o t} e^{-\frac{t^2}{2f^2}} \quad (9)$$

Its Fourier transform with scaled a becomes

$$\hat{\psi}_M(a\,w,\ f) = \pi^{-\frac{1}{4}} e^{-\frac{f^2(a\,w-w_o)^2}{2}} \quad (10)$$

Adaptive Morlet Wavelet Function

To make the adaptive of CMWT, a new parameter q is added to the γ shape parameter. Hence $\gamma(f) = 1/f^q$. The new parameter can control the γ shape parameter of the Morlet wavelet function. The value of q was selected from a set $0<q<1$, when $q=0$ corresponding to equation (4) of Morlet wavelet function and $q = 1$ corresponding to the equation (9) of Morlet wavelet function. By calculating an optimal value of q i.e. say ($q_{opt.}$), the maximum energy concentration (ECMmax) can be obtained. Method to find $q_{opt.}$ has been discussed in the section entitled ***Algorithm to Determine*** $q_{opt.}$. Thus, adaptive Morlet wavelet function and its Fourier transform becomes

$$\psi_M(t,\gamma(f)) = \pi^{-\frac{1}{4}} e^{-iw_o t} e^{-\frac{t^2}{2f^{2q}}} \quad (11)$$

$$\hat{\psi}_M(a\,w,f) = \pi^{-\frac{1}{4}} e^{-\frac{f^{2q}\,(a\,w-w_o)^2}{2}} \quad (12)$$

If adaptive Morlet wavelet function put in place of mother wavelet ψ(t), then standard CMWT is known as ACMWT.

Power Spectra of Adaptive Continuous Morlet Wavelet Transform

Wavelet transform is a complex time-frequency analysis method of signals, so the transform have real as $R(W_{ACMWT})$ imaginary part as $Im(W_{ACMWT})$ and amplitude calculated as $|W_{ACMWT}| = \sqrt{R(W_{ACMWT})^2 + Im(W_{ACMWT})^2}$ and the power of spectra is defined as $|W_{ACMWT}|^2$.

Algorithm to Determine q_{opt}

The determination of q_{opt} depends on energy concentration measurement (ECM). The q_{opt} value of q can be determined by two ways, one is to determine a global method, in which value of q invariant for entire signal. The other is to determine a value of q which is varying with time instant considered [22, 34]. In this paper, we have applied global method for selecting q_{opt}. Advantage of this method is to give exceptional temporal and spectral resolution. The ECM is defined as:

$$ECM(q) = \frac{1}{\iint_{-\infty}^{+\infty} \overline{T^q(t,f)} dt\, df} \quad (13)$$

Symbol $T^q(t,f)$ is used for any time-frequency transform (like ACMWT, AST and AMST) for a value of q. The normalized energy $\overline{T^q(t,f)}$ defined as

$$\overline{T^q(t,f)} = \frac{T^q(t,f)}{\sqrt{\iint_{-\infty}^{+\infty} |T^q(t,f)|^2\, dt\, df}} \quad (14)$$

The algorithm of global method applied in this study is presented in Figure 1.

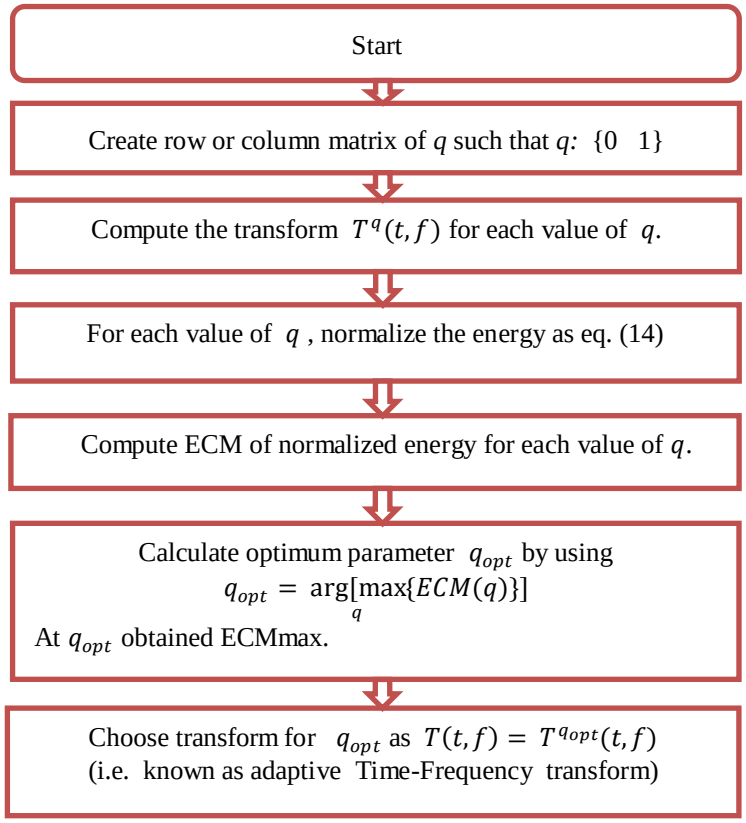

Figure 1. Flow chart of the applied algorithm

Statistical Analysis

Statistical analysis was performed using t-test for comparison of LFp, HFp and LFp/HFp ratio values (taken median of interquartile values) between healthy young group (HEG) subject and healthy elderly group (HEG), arrhythmia controlled medication group (ARCMG) and supraventricular tachycardia group (SVTG) subjects. All p-values were calculated using one-tailed t-test method at $p<0.05$ and considered statistically significant. Results are reported as mean±Sd. The ECMmax of individual synthetic characteristics of HRV signals was calculated at α= 5% without noise and SNR= 30 dB for each considered time-frequency transform (TFT) methods.

Materials

Synthetic Test Signals

As in Table 1, to validate the capability of considered TFT methods for exceptional temporal and spectral resolution in terms of ECMmax, we have generated four synthetic signals sampled at 4Hz and in the duration of $0 \leq t \leq 300$ sec. The synthetic signals are listed in Table 2. The characteristics (stationary and non-stationary) of synthetic signals were modeled as individual physiogomies of HRV

signals. The instantaneous frequency of each component of synthetic signals is determined by $f(t)=(d\emptyset)/(2\pi dt)$, here $\emptyset$ is angle of each cosine component of synthetic signals. The stationary characteristics of synthetic signal related to Mayer - wave (around 0.1Hz in LF band) and respiratory sinus arrhythmia (RSA) (around 0.4 Hz in infant or 0.25 in HF band) [35]. All the possible non-stationary characteristics like all possible frequency range of sympathetic and parasympathetic activity (i.e. increased or decreased the heart rate) and respiratory frequencies observed in many autonomic tests has been covered in the used non-stationary model in this study [36]. The change in heart rate depends on factors such as the person's activity level, posture, recent diet, degree of fitness, age and health [37]. From a theoretical viewpoint, the tracking of time varying, slow or fast spectral components of HRV signals characterized by sinusoidal frequency modulation is challenging due to the high level of inner interference among signals with such a modulation[38]. In this situation, separating LFp and HFp components of HRV signals requires high ECM or resolution and applied method should follow the ideal time-frequency mapping.

Table 1. Morlet wavelet function, S-Transform function and their time domain, Fourier transform time-frequency resolution factor and Scale to frequency Fourier factor

Estimator	Time Domain	Fourier transform	Resolution factor	Scale to freq. factor
Morlet wavelet function	$\pi^{-\frac{1}{4}} e^{-iw_o t} e^{-\frac{t^2}{2}}$	$\pi^{-\frac{1}{4}} H(w) e^{-\frac{(aw-w_o)^2}{2}}$ with scaled 'a'	*a*	$\frac{4\pi a}{w_o+\sqrt{2+w_o^2}}$
Adaptive Morlet wavelet function	$\pi^{-\frac{1}{4}} e^{-iw_o t} e^{--\frac{t^2}{2f^{2q}}}$	$\pi^{-\frac{1}{4}} H(w)\, e^{-\frac{f^{2q}\,(a\,w-w_o)^2}{2}}$ with scaled 'a'	a, f and q	$\frac{4\pi a}{w_o+\sqrt{2+w_o^2}}$
Adaptive ST function	$\frac{\lvert f\rvert^q}{\sqrt{2\pi}} e^{--\frac{f^{2q}t^2}{2}}$	$e^{-\frac{2\pi^2 v^2}{f^{2q}}}$	f and q, When q =1 then ST function.	Not Applicable
Adaptive Modified ST function	$\frac{\lvert f\rvert}{(\frac{1}{N} f + q\ var(sign.))\sqrt{2\pi}} e^{-x}$ $x=\frac{f^2 t^2}{2(\frac{1}{N} f+q\ var(sign.))^2}$	$e^{-\frac{2\pi^2(\frac{1}{N} f+q\ var(sign.))^2 v^2}{f^2}}$	f and q	Not Applicable

H(w) is a Heaviside step function used for analytical wavelet , {H(w)=1 if w>0 ,H(w)=0 otherwise }

Standard Database and Pre-processing of HRV Signals

In this study, the data used in the analysis was obtained from physioNet ATM [39]. The database of 28 healthy subjects, in which 14 HYG (7M+ 7F, age range 23-32) and 14 HEG (7M+7F, age range 70- 82) from the standard Fantasia database sampled at 250 Hz[40], the database of 14 ARCMG subjects (6M+ 8F, age range 54-70) from MIT-BIH arrhythmias sampled at 360 Hz and the 14 SVTG subjects (6M+8F, age not defined) from MIT-BIH supraventricular arrhythmia database sampled at 128 Hz [41, 42] has been used. The R peaks of the ECG signal were detected using modified Tompkins's algorithm [43]. The modified "Pan and Tompkins" QRS detection algorithm locate the QRS complexes depending on digital analysis of amplitude, width, and slope of the ECG signals. This algorithm uses special digital band pass filter to reduce the false detection. The automatic thresholds adjustment mechanism adapts to the morphology variation of the ECG signals. The algorithm follows the steps (i) Band pass filtering. (ii) Differentiation (iii) Squaring (iv) Moving window integration and (v)Thresholds adjustment. From this detected R peaks, R-R interval also known as inter beat interval (IBI) time series has been computed.

Pre-processing of IBI time series data is required before analysis of HRV signal to reduce error and enhance the sensitivity of time series data. First, we have done ectopic beat or interval detection, correction and resampling before HRV analysis. In this paper, the ectopic beats were detected on the

basis of standard deviation filter method which marks outliers as being intervals that lie outside the overall mean IBI by a user defined value of standard deviation [44]. The user-defined value was used as 3 times of standard deviation. A cubic spline interpolation method was used to replace ectopic intervals founded during the detection process. After replacing R-R intervals (second), now it is known as normal-to-normal intervals (NN intervals) [45]. By using cubic spline method the NN intervals were resampled at 4 Hz.

Table 2. Example of synthetic test signal and their characteristics and Sampling frequency (Fs), duration of signals

Experiment	Synthetic test signal	Characteristics	(Fs) and duration
1	$Y_1(t)=\begin{cases}\mathrm{Cos}(0.2\pi t) & 0 \le t < 60\ Sec \\ 0 & 60 \le t \le 180\ Sec. \\ \mathrm{Cos}(0.8\,\pi t) & 180 < t \le 300\ Sec.\end{cases}$	Stationary	$Fs = 4$Hz, and $0 \le t \le 300\ Sec.$
2	$Y_2(t) = Cos(0.518\pi t + 183\pi \times 10^{-6} t^2) + Cos(0.0392\pi t - 261\pi \times 10^{-7} t^2) + Cos(0.118\pi t + 784\pi \times 10^{-7} t^2)$	Non-stationary and slowly time varying spectral components	$Fs = 4$ Hz, $0 \le t \le 300\ Sec.$
3	$Y_3(t) = Cos\left[\left\{0.168\pi\left(\frac{t-150}{300}\right)\tan^{-1}\left(\frac{21t-3150}{300}\right)\right\} - \left\{\frac{0.082\pi \log((21t-3150)^2+1)}{63\times 10^4}\right\} + 0.50\pi t\right] + Cos(0.22\pi t - 206\times 10^{-6}\pi t^2)$	Non-stationary and fast time varying spectral signal	$Fs = 4$ Hz, $0 \le t \le 300\ Sec.$
4	$Y_4(t) = Cos\left(0.078\pi \log\left(\frac{10t+300}{300}\right)\right) + Cos(0.188\pi t + 104\times 10^{-6}\pi t^2)$	Non-stationary and fast frequency variation signal	$Fs = 4$ Hz, $0 \le t \le 300\ Sec.$

Results and Discusion

Simulation Study of Synthetic Signals

Experiment 1

The first signal $Y_1(t)$ is a stationary signal. It consists of two signals having frequency 0.1 Hz and 0.4 Hz in the interval $0 \le t < 60$ sec. and frequency component of 0.4 Hz in interval $180 < t \le 300$ sec. It is analyzed with the CMWT at $w_o = 6$shown in Figure 2.b, ACMWT at $w_o = 6$ (Figure 2.c), ST Figure 2.d, AST Figure 2.e, and AMST in Figure 2.f. As earlier discussed, the ideal TFT should only be contained energy concentration along distributed frequencies for duration of signal components and not cross interfere with neighboring components of signals. The power spectra of ACMWT at $w_o = 6$ for $q_{opt} = 0.81$ follows much closest to the ideal TFT and achieves higher ECMmax and exceptional resolution among the considered TFT estimator, summarized in table 3. The AST provide better ECMmax than CMWT at $w_o = 6$, ST and AMST, and reflect very good resolution in time and frequency both. However, by visual inspection of the time-frequency representation of AST shown in Figure 2.e is not accurately mapped with HF component of 0.4 Hz. It spread the power spectra across 0.4 Hz frequency also. Therefore, AST estimator is only suitable for LF stationary component of HRV signals. While the ACMWT at $w_o = 6$ is suitable for resolution of both stationary components in LF and HF band.

The performance of considered TFT estimator also tested with the signal $Y_1(t)$ in the presence of AWGN with SNR = 30 dB, in order to understand the enhancement capability of ECMmax .The result of performance measured is reported in Table 3. It is concluded that the ECMmax degraded

for all TFT methods, but the ACMWT at $w_o = 6$ still have highest energy concentration among the considered TFT. Thus, from above discussion, the ACMWT at $w_o = 6$ is more appropriate method for assessment of stationary signals whose frequency lies in HRV spectrum range.

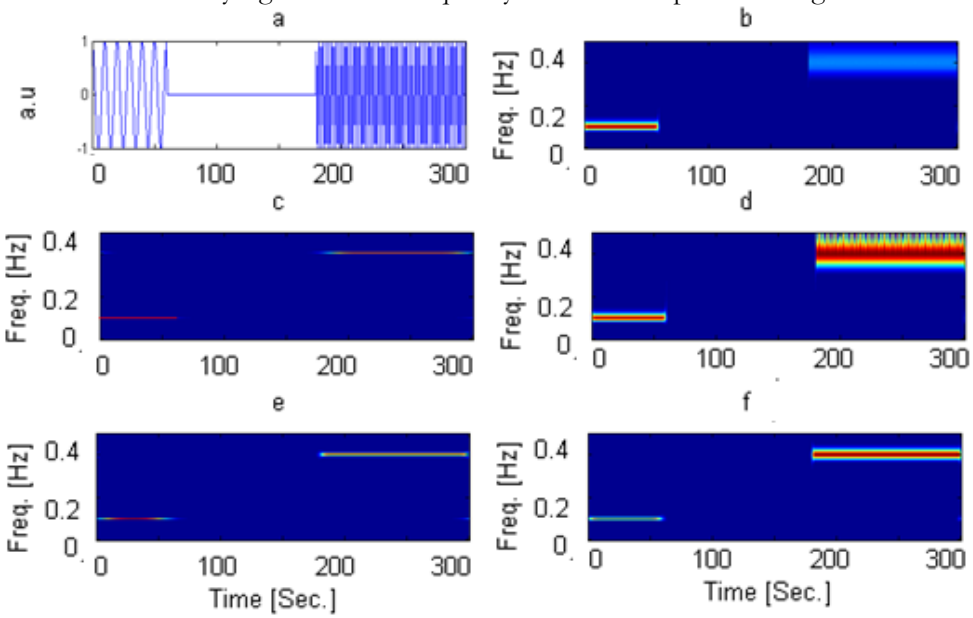

Figure 2. Time-Frequency power spectra maps at statistical significance level at α = 5% of signal (a) time-domain representation of test signal $Y_1(t)$ having arbitrary unit (a.u) amplitude assessed by (b) CMWT at $w_o = 6$ (c) ACMWT at$w_o = 6$ (d) ST(e) AST, and (f) AMST

Table3. The ECMaxvalue of TFT estimator, experiment 1, α=5%

TFT estimator	ECMmax,Noise free	ECMmax, when SNR 30 dB
CMWT	0.0684	0.0630
ACMWT q_{opt}=0.81	0.1796	0.1536
ST	0.0681	0.0636
AST q_{opt}=0.01	0.1546	0.1308
AMST q_{opt}= 0.87	0.0924	0.0837

CMWT = Standard continuous Morlet wavelet transform
ACMWT = Adaptive continuous Morlet wavelet transform
ST = Stockwell transform
AST = Adaptive Stockwell transform
AMST = Adaptive modified Stockwell transform
ECMax =Maximum energy concentration

Experiment 2

The second synthetic test signal $Y_2(t)$ as in Figure 3.a is non-stationary signal and slowly time varying spectra components. It consists of three signals having frequency range (0.26 -0.31 Hz), (0.06 – 0.08 Hz) and (0.018-0.012 Hz). The sampling frequency used is 4 Hz and exists in the interval $0 \leq t \leq 300\ sec$. The power spectra of ACMWT at $w_o = 6$ estimator, shown in Figure 3.c, show clear picture of all three components of signal, either LF or HF band. It is also observed from simulated data, reported in Table 4, it has higher ECMaxcompared to all considered TFT estimator. After the ACMWT at $w_o = 6$method, the AMST depicted as in Figure 3.f has better ECMax (resolution) compared to AST, ST and CMWT at $w_o = 6$. But AMST, AST and CMWT show poor resolution of frequency component signals (0.06- 0.08 Hz, in range of LF band). Hence, the ACMWT at $w_o = 6$ is more appropriate technique, where power spectra of HRV signals varies slowly with time.

Similarly, as in experiment 1, the ECMmax degraded in noisy environment for all TFT method, but ACMWT at $w_o = 6$ estimator for $q_{opt} = 0.31$ still performs better.

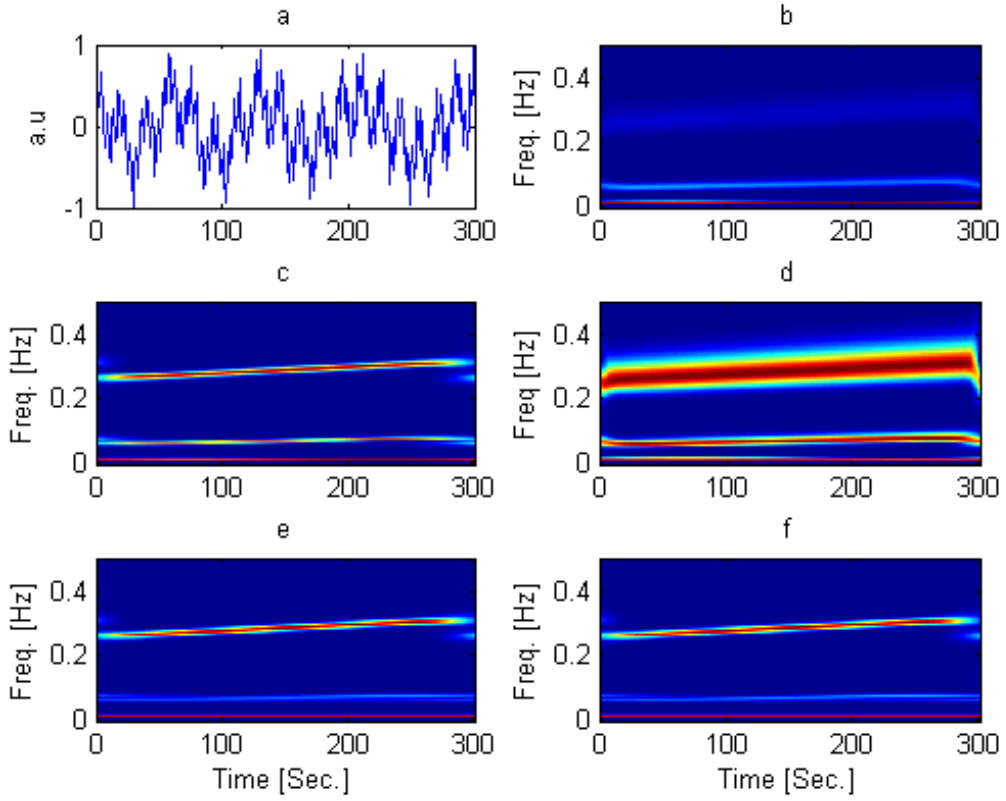

Figure 3. Time –Frequency power spectra maps at statistical significance level at α = 5% of signal (a) time-domain representation of test signal $Y_2(t)$ having arbitrary unit (a.u) amplitude assessed by (b) CMWT at $w_o = 6$, (c) ACMWT at $w_o = 6$, (d) ST, (e) AST, and (f) AMST

Table 4. The ECMmax value of TFT estimator, experiment 2,at α=5%

TFT estimator	ECMmax, Noise free	ECMmax, when SNR 30 dB
CMWT	0.1324	0.1310
ACMWT q_{opt}=0.31	0.1761	0.1705
ST	0.1393	0.1369
AST q_{opt}=0.11	0.1746	0.1675
AMST q_{opt}=0.25	0.1753	0.1681

CMWT = Standard continuousMorletwavelet transform
ACMWT = Adaptive continuousMorletwavelet transform
ST = Stockwell transform
AST = Adaptive Stockwell transform
AMST = Adaptive modified Stockwell transform
ECMax =Maximum energy concentration

Experiment 3

The third synthetic test signal $y_3(t)$ shown in Figure 4.a is non-stationary signal and faster time-varying spectral components. It consists of multiple non-linear components like logarithmic and square functions in first components of signal. The signal was digitized at 4 Hz frequency and exists in the interval $0 \leq t \leq 300\ sec$. The frequency of signal components varies between 0.13-0.4 Hz and 0.048 - 0.11 Hz. The instantaneous frequency of first component signal abruptly changes during 122

-170 sec. The simulated graph of time-frequency representation of AMST for $q_{opt} = 0.21$ and AST for $q_{opt.} = 0.11$ is shown in Figure 4.f and 4.e, has comparable ECMax to ACMWT at$w_o = 6$ as reported in Table 5, It illustrates the clear power spectra of both components of signal $y_3(t)$. However, only upper multiple components have relatively good resolution across 0.4 Hz frequency, while frequency of second component of signal completely fades as time increases. The ACMWT at$w_o = 6$ for$q_{opt} = 0.35$, the time-frequency graph shown in Figure 4.c provides perceptible improvements for all components of signal and achieved higher ECMmax in noise free or in noise compared to all considered TFT estimator, the simulated data are detailed in Table 5.

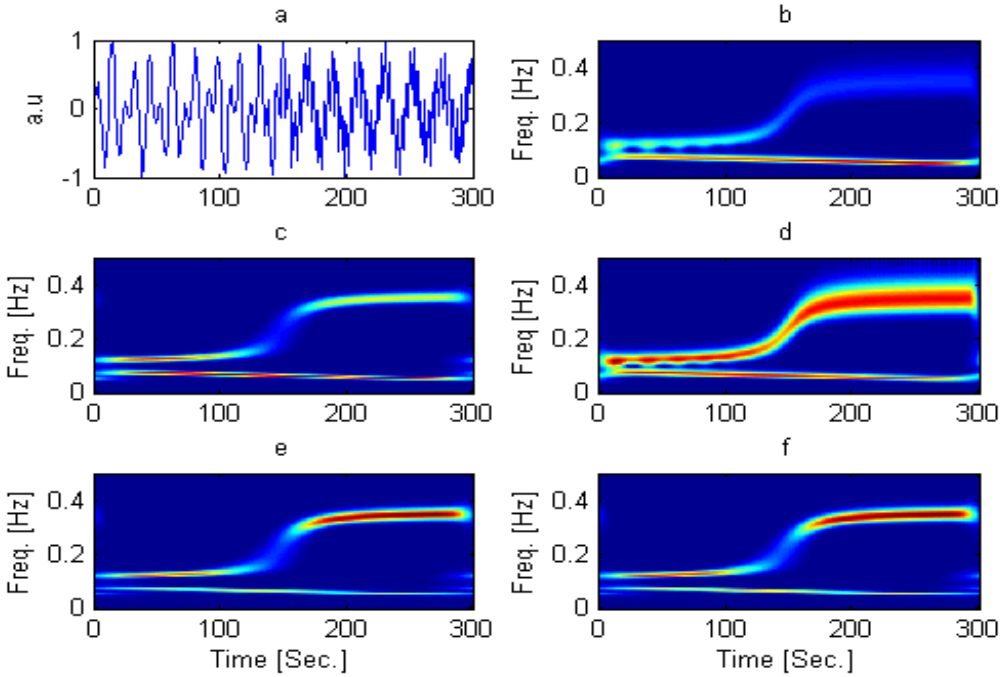

Figure 4. Time –Frequency power spectra maps at statistical significance level at α = 5% of signal (a) time-domain representation of test signal $Y_3(t)$ having arbitrary unit (a.u) amplitude assessed by, (b) CMWT at $w_o = 6$, (c) ACMWT at $w_o = 6$ (d) ST, (e) AST, and (f) AMST

Table 5. TheECMax value of TFT estimator, experiment 3, α = 5%

TFT estimator	ECMmax, Noise free	ECMmax, when SNR 30 dB
CMWT	0.1424	0.1410
AMCMWTq_{opt}=0.35	0.1761	0.1705
ST	0.1393	0.1369
AST q_{opt}=0.11	0.1746	0.1675
AMST q_{opt}=0.21	0.1753	0.1681

CMWT = Standard continuousMorletwavelet transform;
ACMWT = Adaptive continuousMorletwavelet transform;
ST = Stockwell transform; AST = Adaptive Stockwell transform;
AMST = Adaptive modified Stockwell transform

As shown in Figure 4.b and Figure 4.d, the CMWT and ST provides worst resolution for lower signal components, while cross interfere occurs and spread with upper signal component means losing the ideality of time-frequency representation. Thus, from above discussion, the ACMWT at$w_o = 6$ is best estimator for faster time-varying spectral components of HRV signal.

Experiment 4

The last synthetic signal $y_4(t)$ is depicted in Figure 5.a, is one of the important classes of non-stationary signal, in which crossing components exist, that content with fast frequency variation. The

$y_4(t)$ signal is mixture of two signals, one rapidly transiting from lower to higher frequency region (0.04 – 0.4 Hz) and the other linearly varies frequency (0.1 – 0.12 Hz) with time as chirp signal. This signal was sampled at 4 Hz and exists for the duration $0 \leq t \leq 300$ sec. The power spectra of signal $y_4(t)$ was assessed by ACMWT at $w_o = 6$ for $q_{opt.} = 0.21$, is shown in Figure 5.c. The temporal and spectral resolution is excellent up to the crossing component of fast varying frequency component and linear chirp signal. While the resolution after the crossing component of fast varying frequency slightly fades. In spite of this, as the data statement reported in Table 6, the ACMWT at $w_o = 6$ method has better ECMmax compared to other considered method. The AST for$q_{opt.} = 0.30$ is shown in Figure 5.e and AMST for $q_{opt.} = 0.15$ is shown in figure 4.f has better resolution than ST, as in Figure 5.d and CMWT as in Figure 5. b. On the basis of simulated data reported in Table 6, these methods have also ECMmax high compared to the ST and CMWT. Hence, the ACMWT at $w_o = 6$ is best estimator, where power spectra of HRV signals is fast varying with time.

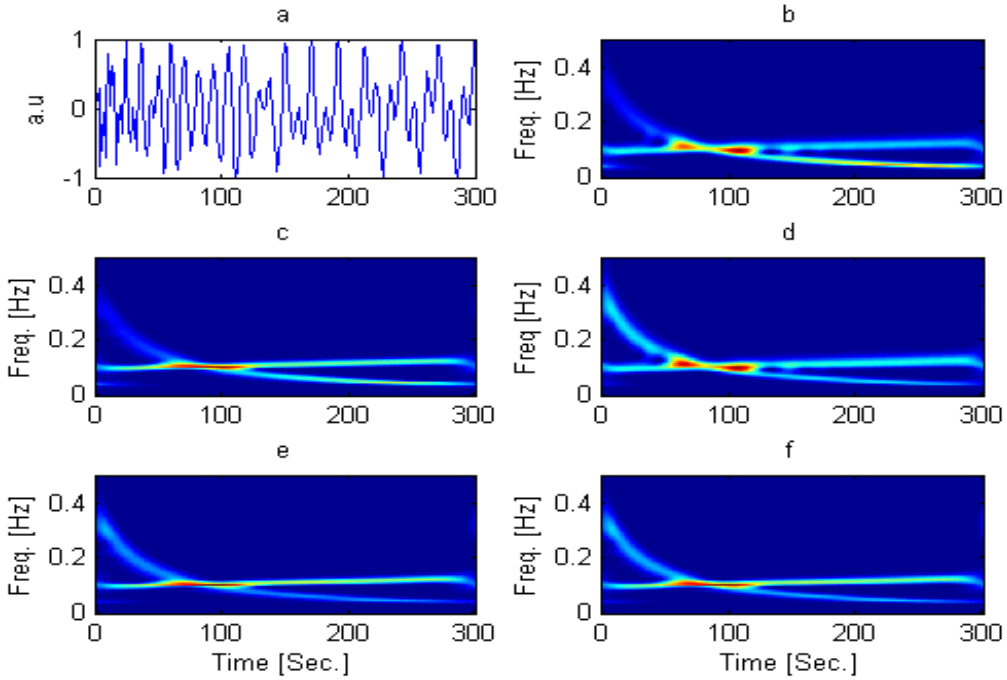

Figure 5. Time- Frequency power spectra maps at statistical significance level at α = 5% of signal (a) time-domain representation of test signal $Y_4(t)$ having arbitrary unit (a.u) amplitude assessed by, (b) CMWT at $w_o = 6$, (c) ACMWT at $w_o = 6$, (d) ST, (e) AST, and (f) AMST

Table 6. The ECMmax value of TFT estimator, experiment 4, α = 5%

TFT estimator	ECMmax, Noise free	ECMmax, when SNR 30 dB
CMWT	0.1757	0.1717
ACMWTq_{opt}=0.21	0.1916	0.1846
ST	0.1736	0.1661
AST q_{opt}=0.30	0.1898	0.1790
AMST q_{opt}=0.15	0.1895	0.1789
CMWT = Standard continuousMorletwavelet transform; ACMWT = Adaptive continuousMorletwavelet transform; ST = Stockwell transform; AST = Adaptive Stockwell transform; AMST = Adaptive modified Stockwell transform;		

Simulation Study of Physiological Signals

The time-frequency power spectra representation obtained from the analysis of HRV of one subject of each group are depicted in Figure 6.

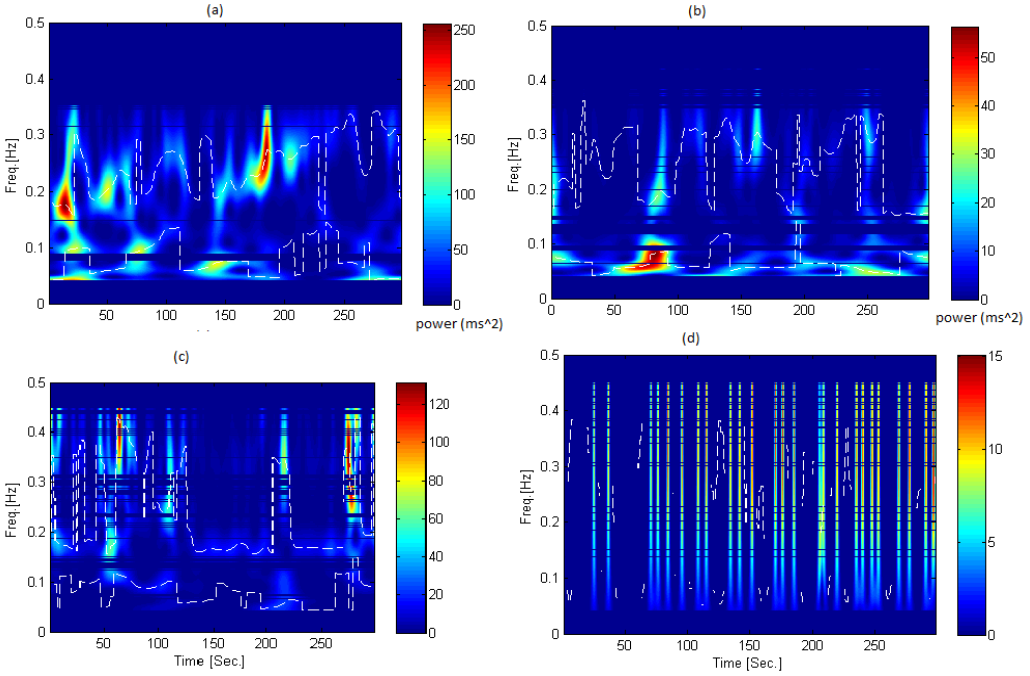

Figure 6. Time-frequency power spectra representation at α = 5% of HRV signals from one (a) healthy young (b) healthy elderly (c) arrhythmia controlled (d) supraventricular tachycardia subject, assessed by ACMWT at $w_o = 6$ estimator, instantaneous frequency are represented by a dotted line in LF and HF band of HRV signals, color bar indicated the index of power (minimum to maximum value in color code) across instantaneous frequency

The time-frequency maps were generated using ACMWT at $w_o = 6$. The instantaneous frequencies (represented as white dotted line on map) of the power spectral components of HRV in LF and HF band, are assessed by localizing the consistent instantaneous spectral peaks [46]. The instantaneous frequencies of the HF components of HRV signal reflect variability of respiratory rate and LF components of HRV are responsible for variability of blood pressure. In healthy young and elderly subjects variability of respiratory rate is high, which fluctuated between 0.15-0.35 Hz and blood pressure variability (0.076±0.012, 0.117±0.016 [47]and 0.1 Hz (Mayer wave) related to baroreflex of control of blood pressure), fluctuate between 0.04-0.15. While variability of respiratory rate and blood pressure in an arrhythmia control subject are slowly fluctuated between 0.16- 0.42 Hz and 0.05 -014 Hz. In case of a supraventricular tachycardia subject, the variability of respiratory rate

and blood pressure are missing for instant and very slowly fluctuated between 0.05-0.12Hz and 0.2 - 0.45 Hz. The color bar represents the index of power (ms^2) content corresponding to instantaneous spectral peaks. The highest index power of color bar is in HRV of young subject approximately 5 times to elderly, 2.4 times to arrhythmia controlled and 16 times supraventricular tachycardia subject. The time-frequency maps of HRV from a young and elderly subject is shown in Figures 6.a and 6.b respectively reflects that the instantaneous power spectral of the HF modulation is lesser than the LF modulation. While in an arrhythmia control subject, shown in Figure 6.c, the instantaneous power spectral of the HF modulation is slightly higher than the LF range. This power spectral of both LF and HF band of HRV signal is very poor in a supraventricular tachycardiac subject, shown in Figure 6.d compared to other subject.

The median trend and interquartile range of spectral indices (LFp, HFp and LFp/ HFp ratio) was estimated from the HRV signal of 14 subjects of each group as shown in Figure 6. While numerical results as average of median trends is given in Table 7. In the calculation of spectral indices, the first and last five samples have been excluded from each group of epoch. The one-tailed t-test method at $p<0.05$ was applied to statistically (p-value) compare the temporal mean values of the spectral indices estimated in each group.

In Figure 7.a, it is shown that the median trend of spectral indices increased in the HYG subjects as compared to other group.

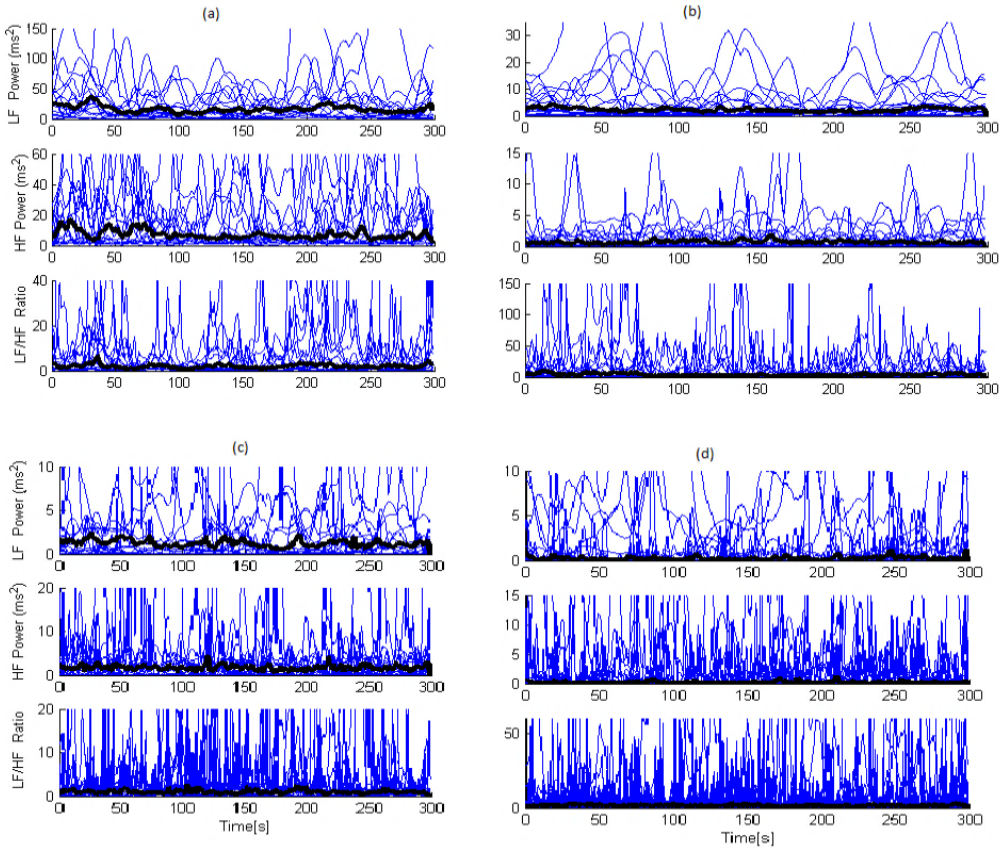

Figure 7. Global results of power spectra indices (in LF, HF band) and LFp/HFp ratio shown as median trend (black line) and interquartile range (blue color) of the HRV signals from all subjects of (a) HYG (b) HEG (c) ARCMG (d) SVTG

The spectral indices LFp/ HFp, which decreases compared to HEG subjects ($p< 0.00001$). In LF an HF band, the average median value as LFp, HFp and LFp/ HFp ratio fluctuated around 16.4019±5.5189, 7.0326±2.7397 and 1.9948±0.8042 in HYG subjects. While these spectral indices altered around 2.2591±0.6405, 0.6974±0.2235 and 3.7655±1.709 in HEG subjects as shown in Figure 7.b. The average median value of LFp/ HFp (3.7655±1.709) was significantly increased

($p<0.0001$) in HEG compared to other group indicating an increased sympathetic activity and decreased vagal activity. However, HFp and LFp was less compared to HYG subjects, it may be caused by significant cardiovascular alterations, both physical as fragility of sinoatrial natural pacemaker cells or of arterial distensibility and functional as changed coupling between regulatory components with aging [48, 49]. From Figure 7.c it can be depicted that the median trend value of LFp and HFp varied around 3.4801±1.1984 and 3.5160±0.9225. These valueswere significantly increased ($p< 0.05$) in ARCMG compared to HEG subjects. It may be due to medication of arrhythmia subject. Drugs like digoxin, pronestyl, norpace and quinidin increases the vigor of myocardial contraction. The increased contractility results in improving the strength of ANS, balancing the cardiac autonomic control system and superficially enhancing cardiac vagal tone in the setting of neuroendocrine stimulation [50, 51, 52]. In comparison to other group subjects, the trend of spectral indices of HRV from SVTG subjects presented in Figure 7.d was characterized by a significant reduction ($p< 0.00001$) in the LFp and HFp component varied around 0.2175±0.1706 and 0.1629±0.1567. As a result, the LF/HF ratio was 1.5677±0.515. It is due to supraventricular tachycardia (SVT) arrhythmia in subjects. During SVT the atria contract against closed atrio-ventricular valves and intra-atrial pressure increases largely. Adjustment of SAN are thus subjected to multiple mechanical surpluses [53]. As a consequence there might emerge weakening of sinus natural pacemaker responses to cyclic changes of strength of signals of ANS with subsequent reducing of LFp and HFp.

Table 7. Global results of power spectra (in LF, HF band) and LFp/HFp ratio, reported as the average of the median trend shown in Figure 7, evaluated for HRV from each group of subjects (first and last 5 samples excluded from the analysis), p-value are statistically significant with respect to the young group subjects at $P <0.05$

Subjects	LF_P (ms^2) (mean±sd)	HF_p (ms^2) (mean±sd)	LF/HF ratio (mean±sd)
HYG Subj.	16.4019±5.5189	7.0326±2.7397	1.9948±0.8042
HEG Subj.	2.2591±0.6405	0.6974±0.2235	3.7655±1.709
ARCMG Subj.	3.4801±1.1984	3.5160±0.9225	0.9634±0.3312
SVTG Subj.	0.2175±0.1706	0.1629±0.1567	1.5677±0.5151
	P≤0.00001		

HYG= Healthy young group; HEG = Healthy elderly group;
ARCMG = Arrhythmia controlled medication group; SVTG = Supraventricular tachycardia group

Extracting meaningful information as LFp and HFp from HRV signals in time-frequency domain is an experimental science [54]. To obtain correct time-varying spectral density, high resolution without any adjacent interference is required. There are various signal processing tools to measure important information from HRV signals in time-frequency domain but for correct analysis the results should be analyzed properly [55, 56]. To test the performance like follow the ideal time-frequency mapping without cross interference, temporal and spectral resolution based on energy concentration of the adaptive methods. They were examined using a set of synthetic individual characteristics of HRV signals.

In first experiment for stationary signal, the depiction obtained by the CMWT at $w_o=6$ contains large cross terms and poor resolution at HF. The ST suffers from the same problem as the CMWT at $w_o=6$, poor frequency resolution at HF and good at LF. AST and AMST methods have better frequency resolution at HF compared to ST and CMWT at $w_o=6$, but it not follows the ideal time-frequency mapping. This was evident that from Figure 1.c, the ACMWT at $w_o=6$ has more uniform resolution and follow the ideal time-frequency mapping at both LF and HF. Therefore, the ACMWT certainly enhances the time-frequency illustration compared to other considered TFT estimator. This result in better energy concentrated time-frequency representation of the stationary signals.

By examining the time-frequency representations of the non-stationary signals like slow and fast time varying spectra components, it can be noticed that the ST and CMWT at $w_o=6$ are capable to internment the LF components but the energy concentration is poor. The illustration was obtained by AST and AMST contains very good resolution for two components same as ACMWT at $w_o=6$,

but frequency component signals (0.06-0.08 Hz, in range of LF band) resolution deteriorate. With the ACMWT more resolution and better energy concentrated time-frequency representation was obtained for all the components of LF and HF, compared to other considered TFT methods.

The time-frequency representation obtained by the ACMWT at $w_o=6$, depicts that spectral components are well energy concentrated up to the crossing of fast varying frequency component and linear chirp signal and diminishes the cross interference. The ST, AST and AMST have good frequency resolution at HF, but, as the frequency (LF) decreases, the temporal and spectral resolution fades. It also surrounds significant cross interference.

From above discussions, it has been concluded that the ACMWT at $w_o=6$ is capable of enhancing the energy concentration of stationary and non- stationary signals in LF and HF band of HRV signals.

Limitations and Future Scope

The ACMWT at $w_o=6$ method is applicable only for (0.02-1Hz) frequency range, not for VLF band. The value of w_o increases the resolution and energy concentration of time-frequency decreases. In this paper, we have studied the energy concentration of HRV time series signals on synthetic as well as standard database of arrhythmia, a future work on wide range of out breaking cardiovascular diseases can act as a bridge between research and clinical practice.

Conclusions

Tests on synthetic simulated signals demonstrate that ACMWT at $w_o=6$ could be an alternative, possibly more effective in terms of energy concentration and resolution, method for assessment of power spectral in HRV time series. Further, the ACMWT at $w_o=6$ has been used for analysis of HRV signals from HYG, HEG, ARCMC and SVTG. By using this method, the median value of interquartile range of spectral indices estimated and compared among group of subjects at statistical significance ($p<0.05$) using t-test method. The global results have depicted that the spectral indices LFp and HFp of HRV are decreased in HEG compared to HYG subjects, it may be due to degrade in autonomic nervous system with aging. While LFp and HFp indices increased in ARCMG compared to HEG subjects, it could be mainly caused by medication of the subjects. The LFp and HFp component of HRV obtained from SVTG are reduced compared to other group subjects. It is due to weak sinus natural pacemaker responses.

Conflict of Interest

The authors declare that they have no conflict of interest.

Acknowledgments

The authors are extremely obliged to the learned reviewers for their helpful comments that significantly improved this paper.

References

1. Roberts-Thomson KC, Lau DH, Sanders P. The diagnosis and management of ventricular arrhythmias. Nature Reviews Cardiology 2011;8:311-21.
2. Tsipouras MG, Fotiadis DI. Automatic arrhythmia detection based on time and time-frequency analysis of heart rate variability. Computer Methods and Programs in Biomedicine 2004;74(2):95-108.
3. Erik S, Sigurd B. Arrhythmia - A Guide to Clinical Electrocardiologye. 1st ed. Publishing Partners; 1991, chapter3.

4. Rao BR. Clinical Electrocardiography. 1st ed. Elsevier Health-INR; 2016. 400 p.
5. Braunwald E, Goldman L, Menz C. Primary Cardiology. 2nd ed. Saunders; 1998. 150-152 p.
6. Khadra L, Al-Fahoum AS, Binajjaj S. A quantitative analysis approach for cardiac arrhythmia classification using higher order spectral techniques. IEEE Transactions on Biomedical Engineering. 2005;52(11):1840-5.
7. Jacobs IG, Oxer HF. A review of pre-hospital defibrillation by ambulance officers in Perth, Western Australia. Medical Journal of Australia. 1990;153(11–12):662-4.
8. Fallen EL, Kamath M V., Ghista DN. Power spectrum of heart rate variability: A non-invasive test of integrated neurocardiac function. Clinical and Investigative Medicine. 1988;11(5):331-40.
9. Wacker M, Witte H. Time-frequency techniques in biomedical signal analysis: A tutorial review of similarities and differences. Methods of Information in Medicine. 2013;52(4):279-96.
10. Witte H, Ungureanu M, Ligges C, Hemmelmann D, Wüstenberg T, Reichenbach J, et al. Signal informatics as an advanced integrative concept in the framework of medical informatics - New trends demonstrated by examples derived from neuroscience. Methods of Information in Medicine. 2009;48(1):18-28.
11. Reed MJ, Robertson CE, Addison PS. Heart rate variability measurements and the prediction of ventricular arrhythmias. Vol. 98, QJM - Monthly Journal of the Association of Physicians. 2005. p. 87-95.
12. Akselrod S, Gordon D, Ubel F, Shannon D, Berger A, Cohen R. Power spectrum analysis of heart rate fluctuation: a quantitative probe of beat-to-beat cardiovascular control. Science. 1981;213(4504):220-2.
13. Pomeranz B, Macaulay RJ, Caudill M a, Kutz I, Adam D, Gordon D, et al. Assessment of autonomic function in humans by heart rate spectral analysis. The American journal of physiology. 1985;248:H151-H153.
14. Electrophysiology TF o. t. ES o. C t. NAS. Heart Rate Variability : Standards of Measurement, Physiological Interpretation, and Clinical Use. Circulation. 1996;93(5):1043-65.
15. Malpas SC, Maling TJ. Heart-rate variability and cardiac autonomic function in diabetes. Diabetes. 1990;39(10):1177-81.
16. Scalvini S, Volterrani M, Zanelli E, Pagani M, Mazzuero G, Coats a J, et al. Is heart rate variability a reliable method to assess autonomic modulation in left ventricular dysfunction and heart failure? Assessment of autonomic modulation with heart rate variability. International journal of cardiology. 1998;67(1):9-17.
17. Sunkaria RK, Saxena SC, Vinod K, Telles S. HRV dynamics in four yogic-based meditation states using optimised AR model. International Journal of Biomedical Engineering and Technology. 2012;9(1):45.
18. Ventosa S, Simon C, Schimmel M, Danobeitia JJ, Manuel A. The S -Transform From a Wavelet Point of View. Signal Processing, IEEE Transactions on. 2008;56(7):2771-80.
19. Stankovic L. An analysis of some time-frequency and time-scale distributions. Annales Des Télécommunications. 1994;49(9–10):505-17.
20. Matz G, Bolcskei H, Hlawatsch F. Time-frequency foundations of communications: Concepts and tools. IEEE Signal Processing Magazine. 2013;30(6):87-96.
21. Orović I, Orlandić M, Stanković S, Uskoković Z. A virtual instrument for time-frequency analysis of signals with highly nonstationary instantaneous frequency. IEEE Transactions on Instrumentation and Measurement. 2011;60(3):791-803.
22. Stankovic L. Highly concentrated time-frequency distributions: Pseudo quantum signal representation. IEEE Transactions on Signal Processing. 1997;45(3):543-51.
23. Gabor D. Theory of communication. J. Institute of Electr. Eng. 1946;93:429-457.
24. Daubechies I. The Wavelet Transform, Time--Frequency Localization and Signal Analysis. IEEE Trans Information Theory. 1990;36(5):961-1005.
25. Mallat SG. A Theory for Multiresolution Signal Decomposition: The Wavelet Representation. IEEE Transactions on Pattern Analysis and Machine Intelligence. 1989;11(7):674-93.
26. Stockwell RG, Mansinha L, Lowe RP. Localization of the complex spectrum: The S transform. IEEE Transactions on Signal Processing. 1996;44(4):998-1001.
27. Stockwell RG. A basis for efficient representation of the S-transform. Digital Signal Processing:

A Review Journal. 2007;17(1):371-93.
28. Lin W, Xiaofeng M. An adaptive Generalized S-transform for instantaneous frequency estimation. Signal Processing. 2011;91(8):1876-86.
29. Assous S, Boashash B. Evaluation of the modified S-transform for time-frequency synchrony analysis and source localisation. EURASIP Journal on Advances in Signal Processing. 2012;2012(1):49.
30. Zhang S, Li P, Zhang L, Li H, Jiang W, Hu Y. Modified S transform and ELM algorithms and their applications in power quality analysis. Neurocomputing. 2016;185:231-41.
31. Liu J, Yao J, Liu X. Generalized S transform with adaptive optimized window and its application in seismic signal analysis. Information Technology Journal. 2013;12(2):276-86.
32. Daubechies I. Ten lectures on wavelets - (C B M S - N S F Regional Conference Series in Applied Mathematics). Society for Industrial and Applied Mathematics SIAM. 1992. p. 377.
33. Belsak A, Flasker J. Adaptive wavelet transform method to identify cracks in gears. Eurasip Journal on Advances in Signal Processing. 2010;2010:879875.
34. Djurović I, Sejdić E, Jiang J. Frequency-based window width optimization for S-transform. AEU - International Journal of Electronics and Communications. 2008;62(4):245-50.
35. Schiecke K, Wacker M, Piper D, Benninger F, Feucht M, Witte H. Time-variant, frequency-selective, linear and nonlinear analysis of heart rate variability in children with temporal lobe epilepsy. IEEE Transactions on Biomedical Engineering. 2014;61(6):1798-808.
36. Orini M, Bailon R, Mainardi LT, Laguna P, Flandrin P. Characterization of dynamic interactions between cardiovascular signals by time-frequency coherence. IEEE Transactions on Biomedical Engineering. 2012;59(3):663-73.
37. Siegel PB, Sperber J, Kindermann W, Urhausen A. Nonstationary time series analysis of heart rate variability. Circulation. 2004;1-10.
38. Boashash B. Note on the Use of the Wigner Distribution for Time-Frequency Signal Analysis. IEEE Transactions on Acoustics, Speech, and Signal Processing. 1988;36(9):1518-21.
39. Moody GB. PhysioNet: Research Resource for Complex Physiologic Signals. Journal of Electrocardiology. 2009;29:1-88.
40. Iyengar N, Peng CK, Morin R, Goldberger AL, Lipsitz LA. Age-related alterations in the fractal scaling of cardiac interbeat interval dynamics. The American journal of physiology. 1996;271(4 Pt 2):R1078-84.
41. Moody GB, Mark RG. The impact of the MIT-BIH arrhythmia database. Vol. 20, IEEE Engineering in Medicine and Biology Magazine. 2001. p. 45-50.
42. Greenwald SD, Patil RS, Mark RG. Improved detection and classification of arrhythmias in noise-corrupted electrocardiograms using contextual information within an expert system. Biomedical Instrumentation and Technology. 1992;26(2):124-32.
43. Pan J, Tompkins WJ. A Real-Time QRS Detection Algorithm. IEEE Transactions on Biomedical Engineering.
44. Mitov IP. A method for assessment and processing of biomedical signals containing trend and periodic components. Medical Engineering and Physics. 1998;20(9):660-8.
45. Ramshur J. Design, Evaluation, and Applicaion of Heart Rate Variability Analysis Software (HRVAS). University of Memphis. 2010;105.
46. Orini M, Laguna P, Mainardi LT, Bailón R. Assessment of the dynamic interactions between heart rate and arterial pressure by the cross time–frequency analysis. Physiol Meas. 2012;33(3):315-31.
47. Kuusela TA, Kaila TJ, Kahonen M. Fine structure of the low-frequency spectra of heart rate and blood pressure. BMC Physiol. 2003;3:11.:11.
48. Voss A, Schroeder R, Heitmann A, Peters A, Perz S. Short-term heart rate variability--influence of gender and age in healthy subjects. PloS one. 2015;10(3):e0118308.
49. Singh D, Vinod K, Saxena SC, Deepak KK. Spectral evaluation of aging effects on blood pressure and heart rate variations in healthy subjects. Journal of Medical Engineering & Technology. 2006;30(3):145-50.
50. Howley ET, Franks BD. Fitness professional's handbook, 5th ed. SciTech Book News. 2007.
51. Zuanetti G, Latini R, Neilson JM, Schwartz PJ, Ewing DJ. Heart rate variability in patients with

ventricular arrhythmias: effect of antiarrhythmic drugs. Antiarrhythmic Drug Evaluation Group (ADEG). Journal of the American College of Cardiology. 1991;17(3):604-12.
52. Brouwer J, van Veldhuisen DJ, Man in 't Veld AJ, Dunselman PH, Boomsma F, Haaksma J, et al. Heart rate variability in patients with mild to moderate heart failure: effects of neurohormonal modulation by digoxin and ibopamine. The Dutch Ibopamine Multicenter Trial (DIMT) Study Group. Journal of the American College of Cardiology. 1995;26(4):983-90.
53. Khayutin VM, Bekbosynova MS, Lukoshkova E V, Golitsyn SP. Spectral analysis of heart rate variability in patients with paroxysmal supraventricular tachycardia. KARDIOLOGIYA. 2001;41(5):38-45.
54. Rajendra Acharya U, Faust O, Adib Kadri N, Suri JS, Yu W. Automated identification of normal and diabetes heart rate signals using nonlinear measures. Computers in Biology and Medicine. 2015;43(10):1523-9.
55. Faust O, Bairy MG. Nonlinear analysis of physiological signals: a review. Journal of Mechanics in Medicine and Biology. 2012;12(4):1240015.
56. Faust O, Prasad VR, Swapna G, Chattopadhyay S, Lim T-C. Comprehensive analysis of normal and diabetic heart rate signals: A review. Journal of Mechanics in Medicine and Biology. 2012;12(5):1240033.